XVIII IMEKO WORLD CONGRESS
Metrology for a Sustainable Development
September, 17 – 22, 2006, Rio de Janeiro, Brazil

INVESTIGATIONS TO THE USE OF SINGLE-CRYSTALLINE SILICON AS MECHANICAL SPRING IN LOAD CELLS

Sascha Mäuselein[1], Oliver Mack[2], Roman Schwartz[3]

[1]Physikalisch-Technische Bundesanstalt, Braunschweig, Germany, Sascha.Maeuselein@ptb.de
[2]Physikalisch-Technische Bundesanstalt, Braunschweig, Germany, Oliver.Mack@ptb.de
[3]Physikalisch-Technische Bundesanstalt, Braunschweig, Germany, Roman.Schwartz@ptb.de

Abstract: This article presents investigation results to the use of single-crystalline silicon as mechanical spring in load cells. As a result of the crystalline structure a very high reproducibility of the material properties is expected. In addition the mechanical aftereffects of single-crystalline silicon are by the factor of 100 smaller than in metallic materials [1]. Performed simulations using the finite element method consider anisotropic and brittle material behavior. It is shown that silicon as mechanical spring material in combination with sputtered metal strain gauges principally can be used for load cells and force sensors.

Keywords: silicon, load cells, force sensors, FEM simulations

1. INTRODUCTION

Generally load cells (LC) and force sensors consist of a metallic mechanical spring applied with several metal foil strain gauges (SG). The strain of the mechanical spring under load is transmitted to the SG. The measurement signal resulting of the change in resistance of the SG is linear to the applied force only in first approximation and shows a more or less high time dependency in form of creep effects. The creep effects are influenced by the material and geometry of the mechanical spring as well as by the material, the geometry and the contacting of the SG. The material of the mechanical spring shows mechanical aftereffects caused by thermal relaxations, atomic diffusion processes and aftereffects in inhomogeneous materials as e.g. movements of dislocations or plastic deformations at grain boundaries, impurities and imperfections. This behaviour is significantly influenced by the thermal and mechanical pretreatment of the material. But even in the case of a good domination of material technology a noticeable scatter of the material properties and of the mechanical aftereffects is unavoidably.

In first approximation the mechanical aftereffects of the spring are compensated by relaxation effects during transmission of the spring's strain to the SG, so called SG creep. Due to multitude of indefinable influence factors the compensation of creep effects is largely based on experimental knowledge and the comprehensive experience of manufacturers. This complicates both the analogue compensation by aligned compensation resistors and the electronic compensation in digital LC by mechatronic systems. On this account load cells conforming highest requirements can be obtained only by sorting. Topically the SG technique is limited by a measuring uncertainty of $2 \cdot 10^{-5}$ (k=2) for SG force transducers and less than 10.000 division values for SG load cells. [2]

The sputtering technique is an alternative procedure to apply SG on mechanical springs. With the sputtering technique the SG material, e.g. NiCr, is vaporised for example by ion bombardment and is deposed on the mechanical spring in form of a thin film. The production of small structures is one of the advantages of this technique. Furthermore the sputtering technique shows negligible SG creep effects compared to conventional glue connections of SG [4]. On the other hand mechanical aftereffects of metallic mechanical springs can not be compensated by this technology. So the sputtering technique has no advantage used in combination with mechanical springs made of metallic materials.

In opposite to metallic materials crystalline materials e.g. silicon (Si) have a defined atomic structure. The material properties of these materials are characterised by constants and are widely independent of thermal and mechanical pretreatment of the material. Synthetic crystal growth procedures (e.g. the floating-zone procedure) allow crystalline materials to be manufactured with very high purity. [3] For Si only the influence of thermal relaxations remain as a matter of mechanical aftereffects [10]. The relative change of elongation due to mechanical aftereffects is by the factor of 100 smaller than in metallic materials and amounts to approximately $5 \cdot 10^{-5}$ [5]. Due to these small mechanical aftereffects a high reproducibility of the strain behaviour is expected.

So Si as crystalline mechanical spring material in combination with sputtered-on metal SG seems to provide advantages compared to SG glued to metallic mechanical springs. A high reproducibility of the measurement signal may be expected and predestines this method to compensate influence factors electronically.

For this reason the development and investigation of LC with mechanical springs made of Si and sputtered-on SG is subject of fundamental research at PTB.

This paper discusses the influence of material behaviour of Si as well as the influence of the geometry of the mechanical spring. The intention is to design a mechanical spring made of Si optimised for the sputtering technique.

The specification of the material properties by exact definable material constants enable to model the behaviour of a crystalline spring analytically and numerically with high accuracy. To model any geometry of the mechanical spring, numerical calculations with the finite element method (FEM) are carried out.

2. MATERIAL PROPERTIES OF SILICON

The simulation of crystalline mechanical springs under load requires the exact knowledge of the subsequently presented material properties of Si.

Si in a single-crystalline structure crystallizes in the cubically surface-centred lattice. The space filling amounts to simply 34% compared to a space filling of 74% in case of the tightest sphere packing. This leads to a smaller density of $2.3 \cdot 10^3$ kg/m^3 than the density of steel ($7.8 \cdot 10^3$ kg/m^3) and aluminium ($2.7 \cdot 10^3$ kg/m^3) (cf. table 1) [2].

Due to direction depending anisotropic material properties of Si the modulus of elasticity is in the range of $13 \cdot 10^{10}$ N/m^2 up to $19 \cdot 10^{10}$ N/m^2 and thus between the value of aluminium ($7.2 \cdot 10^{10}$ N/m^2) and the value of steel ($22 \cdot 10^{10}$ N/m^2). The linear thermal expansion coefficient of Si amounts to $2.5 \cdot 10^{-6}$ 1/K and is by the factor of 10 smaller than the corresponding coefficient of aluminium [4]. Additionally the thermal conductivity of Si is by the factor of 1.5 higher compared to aluminium [6]. Consequently small temperature effects may be expected for mechanical springs made of Si.

Table 1: The most important material parameters.

	density in kg/m^3	module of elasticity in N/m^2	linear thermal expansion coefficient in 1/K
Silicon	$2.3 \cdot 10^3$	$13 \cdot 10^{10}$ to $19 \cdot 10^{10}$	$2{,}5 \cdot 10^{-6}$
Aluminium	$2.7 \cdot 10^3$	$7.2 \cdot 10^{10}$	$24 \cdot 10^{-6}$
Steel	$7.8 \cdot 10^3$	$22 \cdot 10^{10}$	$12 \cdot 10^{-6}$

Up to a temperature of approx. 500 °C single-crystalline silicon deforms purely elastically [4].

Si shows a high hardness and a low fracture stress and thus a brittle behaviour [3]. The Knoop-hardness, comparable with Vickers-hardness but optimized for brittle materials, amounts to 1150 kg/m^3 [4] for Si and is much higher than the hardness of aluminium (approx. 50 kg/m^3) and steel in a range of 100 kg/m^3 up to 400 kg/m^3 (Vickers-hardness) [7]. The values indicated for the fracture stress of Si vary in a large range [8, 9] and are strongly influenced by the surface quality, e.g. micro cracks decrease the fracture stress.

The interrelationship between the stress component σ_λ and strain component ε_μ termed according to the nomenclature defined in [5] is given by the Hook´s law for anisotropic materials

$$\sigma_\lambda = s_{\lambda\mu} \cdot \varepsilon_\mu \,, \qquad (1)$$

whereas $s_{\lambda\mu}$ are the coefficients of a 4th order flexibility tensor. Due to symmetry effects the complete tensor is described by the three values $s_{11} = 7.68 \cdot 10^{-12}$ m^2/N, $s_{12} = -2.14 \cdot 10^{-12}$ m^2/N and $s_{44} = 1.26 \cdot 10^{-11}$ m^2/N [4].

Generally in crystalline materials different directions are described by Miller Indices labelled as (hkl). They identify the different lattice planes. The notation <hkl> with triangular brackets marks the class of equivalent directions which are located perpendicular to the corresponding lattice plane (cf. fig. 1).

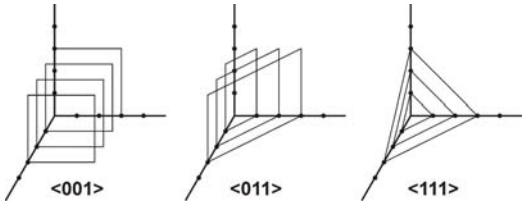

Fig. 1. Important directions in space in silicon illustrated by the lattice planes vertical to them

The formulas in eq. (2) and eq. (3) calculate the modulus of elasticity $E_{[hkl]}$ and the shear module $G_{[hkl]}$ for different orientations of Si labelled in Miller Indices <hkl> [5]:

$$E_{[hkl]} = s_{11} - 2 \cdot (s_{11} - s_{12} - \tfrac{1}{2} s_{44}) \cdot \Gamma \qquad (2)$$

$$G_{[hkl]} = s_{44} + 4 \cdot (s_{11} - s_{12} - \tfrac{1}{2} s_{44}) \cdot \Gamma \qquad (3)$$

with

$$\Gamma = \frac{h^2k^2 + h^2l^2 + k^2l^2}{(h^2 + k^2 + l^2)^2} \,. \qquad (4)$$

The results are shown in table 2 for the most important directions. In the direction <001>, the modulus of elasticity becomes minimal with a value of $13.0 \cdot 10^{10}$ N/m^2, in direction <111> it becomes maximal with $18.8 \cdot 10^{10}$ N/m^2.

Table 2: Elasticity and shear modules for different directions in silicon.

direction in Si	module of elasticity in N/m^2	shear module in N/m^2
<001>	$1.30 \cdot 10^{11}$	$7.96 \cdot 10^{10}$
<011>	$1.69 \cdot 10^{11}$	$6.21 \cdot 10^{10}$
<111>	$1.88 \cdot 10^{11}$	$5.79 \cdot 10^{10}$
<211>	$1.69 \cdot 10^{11}$	$6.21 \cdot 10^{10}$

By assuming a fracture stress of $\sigma_f = 3 \cdot 10^8$ N/m^2 [8, 9] and in consideration of eq. (2) to eq. (4) in direction <001> the fracture strain amounts to $\varepsilon_f = 2.3 \cdot 10^{-3}$. Due to a smaller maximum strain of approximately $1 \cdot 10^{-3}$ of mechanical springs in conventional LC, mechanical springs made of Si are also possible in principle. Admittedly as mentioned above the value σ_f of the fracture stress depends significantly on several effects acting on the surface of Si. Thus e.g. the production process of mechanical springs made of Si affects σ_f in an unpredictable manner and requires additional safety factors if necessary.

3. MECHANICAL SPRING MADE OF SILICON

The following FEM-simulations investigate the strain behaviour of a mechanical spring. Both effects varying geometry parameters as well as the influence of different orientations of Si within the mechanical spring are studied.

The mechanical spring is designed as a double bending beam. This geometry is advantageously for LC. Due to a parallel guidance the strain behaviour of the mechanical spring is largely independent of the point of force introduction.

Furthermore the two thin places of the upper and lower bending beam act as hinges with extension respectively compression under load. By applying SG on the surface of the thin places a full Wheatstone bridge leads to a maximum measurement signal and compensates thermal effects in first approximation.

Figure 2 shows schematically the model of the double bending beam and the parameters to describe the geometry as well as the coordinate system for the orientation of Si.

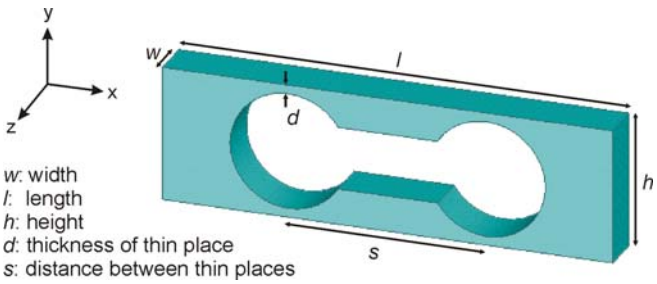

Fig. 2. Geometry and coordinate system of the mechanical spring

The geometry of the double bending beam is given by the length *l*, the height *h* and the width *w*. The thickness of all four thin places is labelled with *d*, the distance between two thin places is termed with *s*.

These parameters are specified to realise optimal strain behaviour under a defined nominal load and in consideration of necessary requirements relevant for manufacturing mechanical springs. Experimental investigations with Si point out, it is very complex to manufacture thin places thinner than 1 mm. Subsequently the geometry is specified for a nominal load of F = 60 N by the following parameters: l = 115 mm, s = 35 mm, h = 30 mm, w = 20 mm and d = 1 mm.

To investigate the influence of orientations of Si within the mechanical spring suitable orientations have to be defined. Thereby the choice of orientations is carried out in consideration of requirements necessary to manufacture mechanical springs made of Si. Because the mechanical springs will be produced out of Si rods grown in the directions <001>, <011> and <111>, the orientations O1 up to O7, shown in fig. 3 are discussed in this paper. Among other things orientations of Si in direction <001> and direction <111> with the lowest respectively highest modulus of elasticity are realisable (cf. table 2).

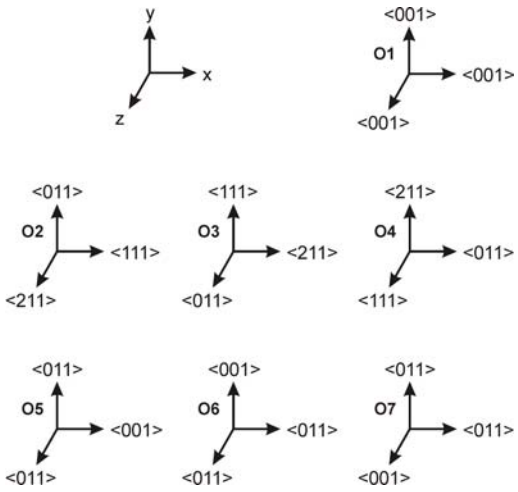

Fig. 3. Investigated orientations of Si within the mechanical spring

For example with orientation O1 and O5 the direction <001> of Si is aligned in x-direction of the coordinate system along the length *l* of the double bending beam. Along the width *w* (z-direction) and the height *h* (y-direction) the Si is aligned in direction <001> for orientation O1 respectively aligned in direction <011> for orientation O5. For orientation O2 the direction <111> of Si is aligned in direction along the length *l* (x-direction), the direction <011> is aligned along the height *h* (y-direction) and the direction <211> is aligned along the width *w* (z-direction). Similar considerations are necessary for the other orientations (see fig. 3).

The modulus of elasticity and the shear module of the orientations O1 up to O7 follow from table 2.

4. SIMULATIONS

Exemplarily fig. 4 shows the strain component ε_x in x-direction shaped in the double bending beam made of Si as a result of numerical simulations carried out with the FEM model according to fig. 2 and under a load of F = 60 N.

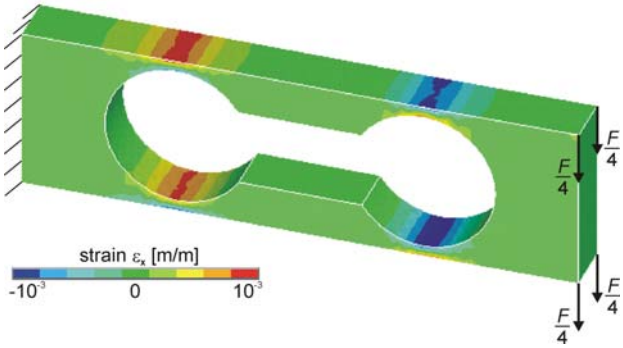

Fig. 4. FEM calculation of a double bending beam made of silicon under a nominal load of F = 60 N

To optimise the geometry and to find the best orientation of Si within the mechanical spring a suitable criterion is necessary. This criterion is the strain to stress ratio

$$r_{ss} = \frac{\varepsilon_{x,max}}{\sigma_{x,max}}, \qquad (5)$$

which describes the maximum strain component $\varepsilon_{x,max}$ at the surface of the thin places in relation to the maximum stress component $\sigma_{x,max}$ of the whole mechanical spring under load. The ratio r_{ss} should be as high as possible to achieve optimal measurement signals.

As expected the thin place surfaces of both the upper as well as the lower bending beam provide areas of maximum extension respectively compression under load. So these areas are predestined to sputter-on SG and to determine the strain to stress ratio r_{ss}.

With regard to this criterion and under the boundary condition not to exceed the fracture stress it is the aim of following investigations to find an optimised geometry and the best orientation of Si for the double bending beam presented in fig. 2.

5. RESULTS

5.1 Different orientations of Si

In consideration of the geometry parameters defined in cap. 3 simulations with different orientations of Si (cf. fig. 2) within the mechanical spring are performed. Initially a nominal force of F = 60 N is applied.

Fig. 6 shows the strain component ε_x at the surface of the upper left thin place as a function of the position x in the range of x = 20 mm up to x = 60 mm. The simulations are carried out for the orientations O1 up to O7 shown in fig. 3.

The strain component ε_x at the upper right thin place shows a similar behaviour but with a negative sign.

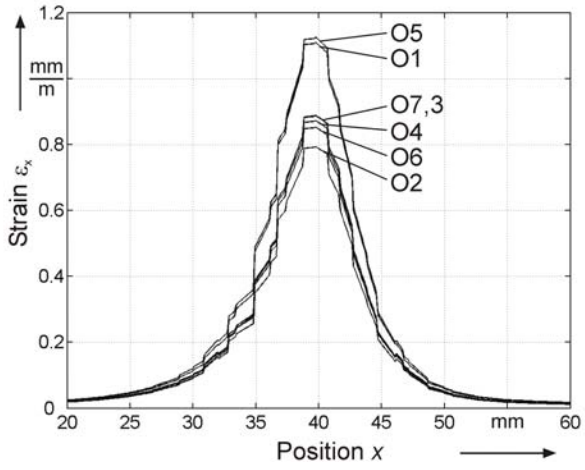

Fig. 6. Strain at the surface of the left thin place under load as function of the position x for different orientations of Si

The investigations result in an orientation depending strain characteristic with maximum strain $\varepsilon_{x,max}$ approximately at $x \approx 40$ mm. The minimum value $\varepsilon_{x,max}$ of all orientations is determined for orientation O2 and amounts to $\varepsilon_{O2,max} = 0.79 \cdot 10^{-3}$. The corresponding maximum strain amounts to $\varepsilon_{O5,max} = 1.13 \cdot 10^{-3}$ for orientation O5 and for this reason it is the preferred orientation. However with a value of $\varepsilon_{O1,max} = 1.11 \cdot 10^{-3}$ orientation O1 also offers a high maximum strain.

These results could be explained in the following way (cf. table 2 and fig. 3): The most important factor for a high maximum strain $\varepsilon_{x,max}$ is a low modulus of elasticity in x-direction. E.g. orientations O1 and O5 have identical modulus of elasticity in x-direction with a lowest possible value of 1.30·1011 N/m^2 determined in direction <001> of Si. The second factor is a low shear module in y-direction. Correspondingly the shear module of orientation O5 (6.21·1010 N/m^2 in direction <011>) is smaller than the shear module of orientation O1 (7.96·1010 N/m^2 in direction <001>).

Furthermore the simulations point out that the maximum strain is not detected exactly in the middle of the thin place at a position of x = 40 mm but in the order of a few mm shifted in direction to the fixed side of the double bending beam. This is important for the later positioning of the SG to achieve best measurement signals.

In the following for the different orientations O1 up to O7 of Si a nominal force

$$F_{OX} = F_{O5} \cdot \frac{\varepsilon_{O5,max}}{\varepsilon_{OX,max}} \tag{6}$$

is calculated in such a manner, that each orientation archive the constant maximum strain $\varepsilon_{O5,max}$ of the orientation preferred. For further clarification table 3 shows the forces F_{OX} analytically calculated according to eq. 6 and the numerically determined maximum stress values $\sigma_{OX,max}$ under the boundary condition of an acting force F_{OX} and for the different orientations O1 up to O7.

Table 3: Nominal force, maximum stress and normalised strain to stress ratio for different orientations with the same maximum strain at the thin place.

orientation	nominal load F_{OX} in N	maximum stress $\sigma_{0X,max}$ in N/m^2	relative strain to stress ratio r_{ss}
O1	60.9	$1.71 \cdot 10^8$	0.99
O2	85.1	$2.41 \cdot 10^8$	0.70
O3	76.1	$2.15 \cdot 10^8$	0.79
O4	77.4	$2.20 \cdot 10^8$	0.77
O5	60.0	$1.69 \cdot 10^8$	1.00
O6	79.2	$2.26 \cdot 10^8$	0.76
O7	76.0	$2.13 \cdot 10^8$	0.79

The investigations point out that for every orientation different from the orientation O5 a force $F_{OX} > F_{O5}$ is necessary to archive the maximum strain $\varepsilon_{O5,max}$ of the preferred orientation O5 which leads to correspondingly large maximum stress values $\sigma_{OX,max} > \sigma_{O5,max}$. These results are also ratified by the relative strain to stress ratio r_{ss} normalised to orientation O5 in table 3. As mentioned above the highest value for relative r_{ss} is achieved for orientation O5. All other orientations reveal smaller values in the range of 1% for orientation O1 up to 30% for orientation O2.

These results demonstrate that the orientation of Si strongly influences the strain behaviour of a double bending beam in a range of a few 10% and consequently influences the measurement signal if SG are applied in experimental applications. The orientations O1 and O5 are most suitable

for experimental realisation whereas all other orientations yield to disadvantageous results.

5.2 Double bending beam geometry

This section deals with the optimisation of the design of the double bending beam shown in fig. 2 with respect to the strain to stress ratio r_{ss} (see eq. 5). Starting from the FEM model defined in cap. 3 (l = 115 mm, s = 35 mm, h = 30 mm, w = 20 mm, d = 1 mm) numerical simulations are carried out with an applied nominal load of F = 60 N and with geometry parameters varied separately within ranges presented in table 4.

Table 4: Ranges of geometry parameters variation.

parameter	range
d	0.2 mm to 4.0 mm
s	20 mm to 50 mm
w	1 mm to 30 mm
h	20 mm to 36 mm

To simplify matters the simulations consider isotropic material properties with a modulus of elasticity of $E = 10^{11}$ N/m^2. This simplification is acceptable because isotropic material properties affect the principle behaviour of the strain to stress ratio r_{ss} as a function of any geometry parameter only marginal as shown in pre-examinations.

Subsequent the effects of geometry parameters variation presented in table 4 are discussed.

Variation of parameter d:

The parameter d describes the thickness of the thin places of the double bending beam (see fig. 2). Figure 8 illustrates both the maximum strain $\varepsilon_{x,max}$ as well as the relative strain to stress ratio r_{ss} as a function of d, whereas r_{ss} is normalised to the strain to stress ratio of d = 1 mm.

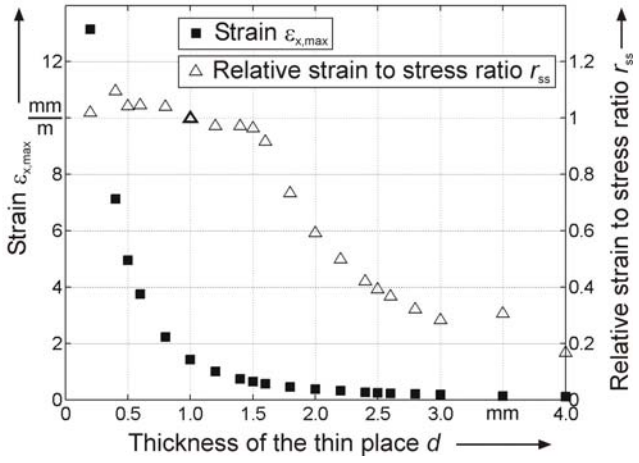

Fig. 8. Left scale: maximum strain $\varepsilon_{x,max}$ right scale: relative strain to stress ratio both as a function of the thickness d of the thin places

As expected the maximum strain $\varepsilon_{x,max}$ decreases - particularly in the range of 0.2 mm ≤ d ≤ 1.5 mm and about more than 90% - with increasing thickness d of the thin places. In this range r_{ss} deliver maximum values widely independent of the thickness d. Only for a thickness d > 1.5 mm r_{ss} also decrease with increasing thickness d. So for d = 4 mm r_{ss} amounts to less than 20% of the initial value determined for d = 1 mm.

So d should be smaller than 1.5 mm for a good strain performance but not smaller than 1 mm due to manufacturing reasons.

As conclusion the investigations point out for the geometry defined the thickness d of the thin places should amount less than 1.5 mm for an optimal strain to stress ratio r_{ss}. However due to requirements relevant for manufacturing double bending beams made of Si the thickness d should amount not less than 1 mm.

Variation of parameter s:

The parameter s determines the distance between the thin places of the upper respectively the lower beam (see fig. 2). The investigations point out a mostly linear interrelationship between an increasing maximum strain $\varepsilon_{x,max}$ and an increasing distance s. The maximum stress $\sigma_{x,max}$ shows the same linear interrelationship in principal.

So the variation of the strain to stress ratio r_{ss} only amounts to 10% in the simulation range of 20 mm ≤ s ≤ 50 mm. Therewith the influence of the parameter s on the strain performance is negligible in respect to parameter d.

For this reason to achieve best fracture properties the thickness d of the thin places should be dimensioned in aspect of a maximum strain to stress ratio r_{ss}. The distance s between the thin places should be dimensioned concerning the nominal load required. However it has to be noticed advanced simulations show a decreasing natural oscillation frequency with decreasing s. So the distance s can not be arbitrary long for a suitable dynamic behaviour.

Variation of parameter w:

The parameter w identifies the width of the double bending beam (see fig. 2). Figure 9 shows the maximum strain $\varepsilon_{x,max}$ as well as the relative strain to stress ratio r_{ss} as a function of w, whereas r_{ss} is normalised to the strain to stress ratio of w = 20 mm.

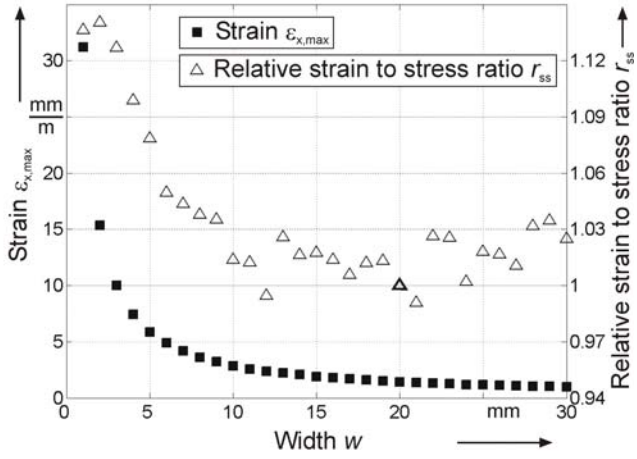

Fig. 9. Left scale: maximum strain $\varepsilon_{x,max}$ right scale: relative strain to stress ratio both as a function of the width w

The maximum strain $\varepsilon_{x,max}$ decreases with increasing width w. In the range of 1 mm ≤ w ≤ 5 mm the decreasing amounts to 85% whereas relative r_{ss} deliver maximum values of approximately 1.1. Within 5 mm ≤ w ≤ 30 mm $\varepsilon_{x,max}$ decreases about 15% and r_{ss} is widely independent of the width w.

Although r_{ss} is approximately 10% higher in the first range, values of w < 10 mm are not suitable for the aspired nominal load due to difficult manufacturing processes in such a width range. In the range of interest (w > 10 mm) the parameter w is widely negligible concerning its influence on the strain to stress ratio r_{ss}. So the width w can be used as well as the distance s between the thin places to design the double bending beam with regard to the suitable nominal load.

Variation of parameter h:

The parameter h describes the height of the double bending beam (see fig. 3). As expected for the investigations carried out the maximum strain $\varepsilon_{x,max}$ and the maximum stress $\sigma_{x,max}$ are mostly independent of h. Accordingly in the range of 20 mm ≤ h ≤ 36 mm r_{ss} vary in a small interval about 2.7%. For this reason the height h can be designed concerning the requirements of manufacturing processes primarily.

7. CONCLUSION AND OUTLOOK

This paper presents first results of investigations for using single-crystalline silicon as mechanical spring material in load cells. As a result of the crystalline structure of this material a very high reproducibility of the material properties is expected. In addition the mechanical aftereffects of single-crystalline silicon are by the factor of 100 smaller than in metallic materials [1].

Therefore silicon as crystalline mechanical spring material in combination with sputtered-on metal strain gauges seems to provide advantages compared to strain gauges glued to metallic mechanical springs. A high reproducibility of the measurement signal is expected and predestines this method to compensate influence factors using electronically methods.

This contribution discusses both the influence of different orientations of silicon within the mechanical spring as well as the influence of varying geometry parameters. The investigations are carried out with numerical models and the finite element method. Therefore the mechanical spring is modelled as a double bending beam. Due to a parallel guidance the strain behaviour of this geometry is largely independent of the point of force introduction.

The investigations of varying geometry parameters point out the thickness d of the thin places of the double bending beam should be less than 1.5 mm for an optimal strain to stress characteristic. A limiting factor is the manufacturing process of mechanical springs made of silicon allowing thin places with a minimum thickness of 1 mm.

The distance s between the thin places and the width w do not affect the strain to stress ratio significantly and thus are negligible in the geometry parameter range of interest. Admittedly these parameters are useful for dimensioning the load cell concerning the required nominal load.

The anisotropic material properties of silicon permit different orientations within the mechanical spring. Admittedly the influence of these orientations concerning the strain behaviour of a double bending beam is widely unknown up to now. The numerical investigations result a significant dependency between the orientation of silicon and the strain behaviour at the thin places of the double bending beam in a range of approximately 30%. Particularly the orientations O1 and O5 (see fig. 3) are the preferred orientations with a maximum strain to stress ratio.

The experimental realisation of the double bending beam considering the results of numerical simulations carried out in this paper is the subject of developments in the near future. Particularly the orientation of the silicon within the mechanical spring will be taken into account. Furthermore safety factors of the geometry parameters have to be used to avoid fracture failure which strongly depends on the surface quality of silicon material.

REFERENCES

[1] Baumgarten, D., “Bestimmung der elastischen Nachwirkung von Metallischen und Nichtmetallischen Federwerkstoffen im Kriechversuch”, *Dissertation*, Braunschweig, 1989

[2] Mäuselein, S., Schwartz, R., “Alternative Sensoren für die Wägetechnik”, *50. Internationales Wissenschaftliches Kolloquium der Technischen Universität Ilmenau*, Series 5.1, September 2005

[3] Weißmantel, Ch., Hamann C., „Grundlagen der Festkörperphysik”, Leipzig, 1995, ISBN 3-335-00421-3

[4] Büttgenbach, S., “Mikromechanik”, Teubner Studienbücher, Stuttgart, 1991, ISBN 3-519-034071-3

[5] Over, H.-H., “Elastische und plastische Eigenschaften von einkristallinem Silicium in Abhängigkeit von der Temperatur und der Versetzungsdichte”, *Dissertation*, Aachen, 1977

[6] “Formeln und Tabellen für die Sekundarstufen I und II”, *Formelsammlung*, Paetec, 1994

[7] Fischer, U., “Tabellenbuch Metall”, Haan-Gruiten, 2005, ISBN 3-8085-1723-9

[8] Gmelin, “Gmelins Handbuch der anorganischen Chemie, Silicium”, Verlag Chemie, Weinheim, 1959

[9] Saif, M., “Micro Mechanical Single Crystal Silicon Fracture Studies”, IEEE, 1996

[10] Mack, O., “Verhalten piezoelektrischer Kraftaufnehmer unter Wirkung mechanischer Einflussgrößen”, *Dissertation*, Braunschweig, 2006